A Platinum Open Access Journal for Organic Chemistry

Paper

Free to Authors and Readers | DOAJ Seal | *Arkivoc* **2024** (3) 202412258

Studying the formation and the final structure of AuPt bimetallic systems by cyclic voltammetry

M. Stucchi, I. Barlocco, A. Villa, V. Pifferi, L. Falciola, and L. Prati*

Dipartimento di Chimica, Università degli Studi di Milano , via Golgi 19, 20133 Milano, Italy
Email: laura.prati@unimi.it

Received 07-17-2024 **Accepted** 09-10-2024 **Published on line** 09-19-2024

Abstract

Currently, bimetallic nanosystems are some of the most promising materials for catalytic, electrocatalytic and electroanalytical applications, thanks to their novel optical, catalytic, magnetic and sensing properties. However, their characterisation is still a challenge in terms of both the type and the quantity of the metal involved and their structure (e.g. alloyed or core-shell). It is also important to note that these systems underwent modification in time due to the mobility of atoms and the drive to reach the most stable thermodynamic status. In this work, we suggest cyclic voltammetry as a convenient technique for the study of bimetallic nanocomposites and their evolution during the synthetic process. In particular, Pt+Au, Au@Pt and Pt@Au systems have been deeply investigated by comparing their voltammetric results in terms of the shift in the Au and Pt peak potentials and absence/presence of some peaks. Furthermore, the samples were studied with TEM analysis. The results allowed for the discrimination of alloyed and core-shell structures and provided a method to follow changes in the composites during their synthetic preparation. It also enabled the deep analysis of how the two metals interact each other, thereby yielding the peculiar properties that are conveniently used for catalytic purposes.

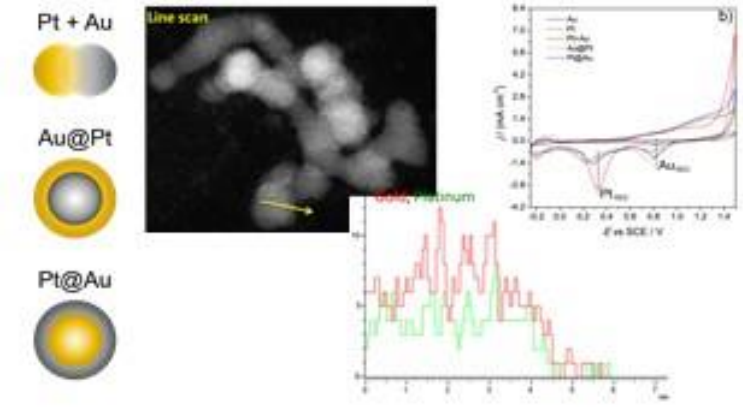

Keywords: Bimetallic nanoparticles; Pt nanoparticles; Au nanoparticles; cyclic voltammetry; alloy; core-shell.

Cite as *Arkivoc* **2024** (3) 202412258
DOI: https://doi.org/10.24820/ark.5550190.p012.258

Introduction

Over the last decades, a lot of attention has been devoted to the understanding of the chemical behaviour and the peculiar properties of systems prepared by the combination of different metal nanoparticles.[1–3] In particular, bimetallic systems have become more frequently investigated due to their novel optical, catalytic, magnetic and sensing properties that often differ from the ones of their monometallic components.[4–10] In this context, it is important to fully characterize and explore these fascinating systems by studying the size, shape, composition and functionalization of the nanocomposites, in order to design sophisticated materials properly adapted to their intended application.[11–17] Beside the type and the quantity of the two metals involved in the bimetallic material, it is important to investigate the morphological distribution of the components, i.e. to discriminate among alloy or core-shell structures.[18–20] Usually, HR-TEM and EXAFS are the conventional techniques commonly involved for the characterization of these systems, because they can provide information about the fine structure of the material.[21–23] However, they suffer from the problems of being very expensive and not so easily accessible, particularly for the initial surveys of the systems.[24–27] In the last decade, electrochemical techniques have been used as alternatives to characterize these bimetallic systems, starting from simple cyclic voltammetry (CV), up to the use of underpotential deposition and nano impact techniques. In this context, cyclic voltammetry certainly remains the easiest to use, low-cost and fastest complementary technique to discriminate amongst alloys and intact or defective core-shell structures.[27-30] The present results presented here however, are focused on the study of the materials after their synthesis[31-33]. A remaining challenge is the possibility to follow the formation morphology of these nanomaterials during their synthesis and its possible evolution after an aging period (or storage). In this work we propose CV as a fast, easy and low-cost technique to also study with time the evolution of the morphology of Au-Pt bimetallic systems during their formation. We directly studied the nanoparticles during their colloidal synthesis, thus avoiding the use of supporting materials which in turn could modify and interfere with the structure evolution. The opportunity to know how the bimetallic structure changes during the synthesis is one of the novel aspects of this work. The results pave the way to the study of analogous gold-based bimetallic systems, to be conveniently involved in catalysis, electrocatalysis and electroanalytical applications.

Results and Discussion

Electrochemical characterization of mono and bimetallic systems

In our previous study, we employed three different preparation methods for the synthesis of AuPt bimetallic systems, in order to obtain an alloy (Pt+Au) and two core-shell (Au@Pt and Pt@Au) structures (Figure 1a).[34–36] However, gold, for its thermodynamic properties is reported to normally tend to migrate to the surface of the systems.[37] Therefore, the real structure of these NPs has not been disclosed yet. Therefore, a preliminary CV screening allowed us to understand the real types of structures produced because of different synthetic approaches (Figure 1b).

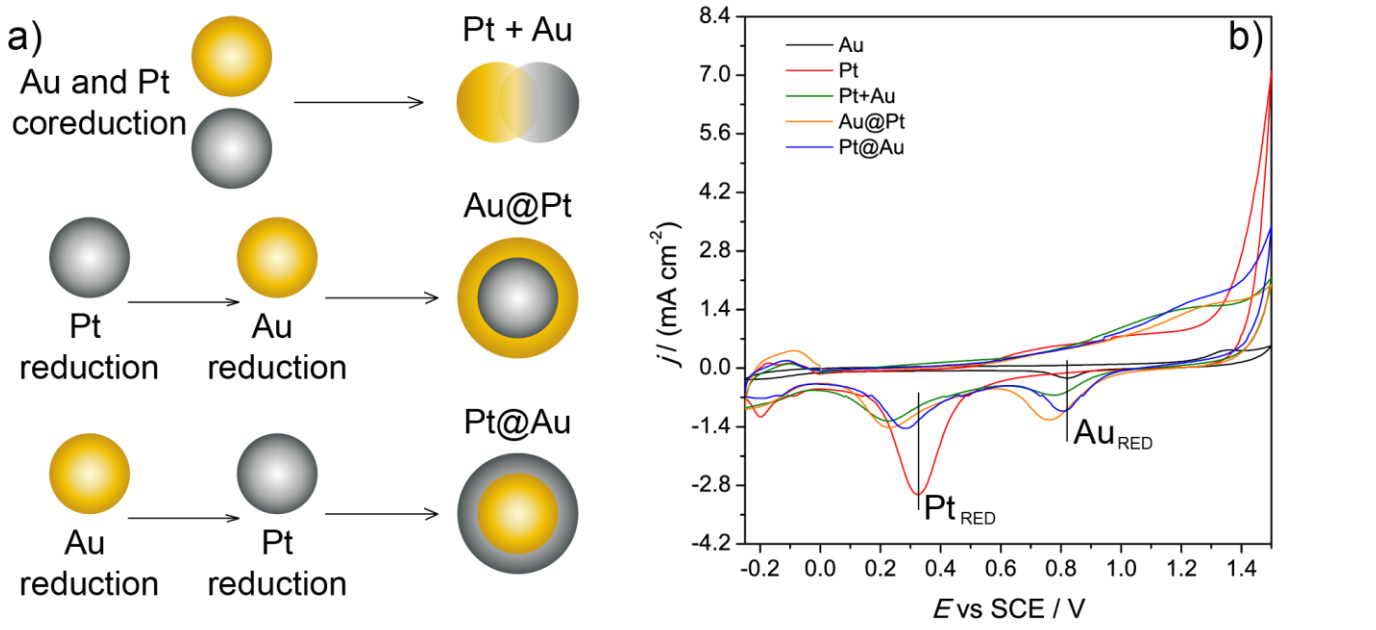

Figure 1. (a) A schematic representation of the expected morphology of the samples. (b) CV of the three bimetallic systems (Pt+Au, Au@Pt and Pt@Au) and the relative monometallic Au and Pt components, recorded at 100 mV s^{-1} in 0.1 M H_2SO_4 after 48 h.

The voltammetric behaviours of both Pt and Au monometallic sols are also reported for comparison. Observing the voltammograms of bimetallic nanoparticles, a broad oxidation plateau in the anodic region can be seen. This signal, approximatively between 0.9 and 1.3 V (SCE), comprises the oxidation of both platinum and gold nanoparticles, even though in the monometallic samples the peaks are very weak. On the contrary, in the cathodic region, two different reduction peaks for all the bimetallic systems can be clearly distinguished. These peaks refer to the disruption of gold (at around + 0.8 V (SCE) – very small for monometallic Au) and platinum oxide (at around + 0.3 V (SCE)- very strong for monometallic Pt), respectively. Comparing the position of the reduction peaks (Table 1), it is evident that (Pt+Au) and (Au@Pt) systems behave almost in the same way, showing positions of the reduction peaks both cathodically shifted with respect to the ones of the monometallic Au (Au_{RED})and Pt (Pt_{RED}) counterparts.[38] We associate these differences to a variation of reducibility/oxidizability of the metals. The cathodic shift of the reduction peaks in these bimetallic systems suggested a stabilization of both oxides in the composite. This stabilization might be due to the intimate contact between the components, which results in a general enrichment of electrons in the oxide forms. In particular, Pt in these systems is more stabilised (ΔE = 100 mV) with respect to Au (ΔE = 30-50 mV), suggesting an electron donation from Au to Pt. In other words, we believed these variations in CV peaks are compatible with the conclusion that Au+Pt and Au@Pt NPs behave like an alloy where there is an intimate contact between Au and Pt, with properties slightly different from the correspondent metal components. However, the chemical behaviour of Au or Pt external shell is expected to be different, with Pt being more prone to oxidation.

Pt@Au sample showed, on the contrary, an intermediate behaviour: similar to monometallic in the Au region while shifted in the Pt one. In this case, the reduction peak of gold is practically the same as in the case of monometallic, while the platinum one shows a slight shift (ΔE = 40 mV) with respect to the monometallic counterpart. Following the same line as in the other two cases, we concluded that in Pt@Au, differently from Au+Pt and Au@Pt, the two metals appear to be less close to each other, with Au showing no donation toward

Pt and thus preserving its identity. These observations can suggest a possible partial segregation of the materials.

Table 1. Reduction potential values at 0.1 V s^{-1} of the bimetallic and monometallic systems. $\Delta E = E_{monometallic} - E_{bimetallic}$

Electrode	E (Au_{RED}) / V	ΔE (Au_{RED}) / V	E (Pt_{RED})/ V	ΔE (Pt_{RED}) / V
Au	0.82	-	-	-
Pt	-	-	0.33	-
(Pt+Au)	0.79	-0.03	0.23	-0.10
(Au@Pt)	0.77	-0.05	0.23	-0.10
(Pt@Au)	0.82	0.00	0.29	-0.04

HR-TEM Characterization of bimetallic systems

The information gained from the voltammetric patterns were also compared with the results obtained from HR-TEM analyses. High annular dark-field scanning transmission electron microscopy (STEM-HAADF) images showed AuPt nanoparticles with a mean diameter in the range of 3-4 nm in all cases (Figure 2). Furthermore, energy-dispersive X-ray spectroscopy (EDX) analyses from individual particles confirmed that the majority of nanoparticles were bimetallic AuPt in nature, for all the three systems.

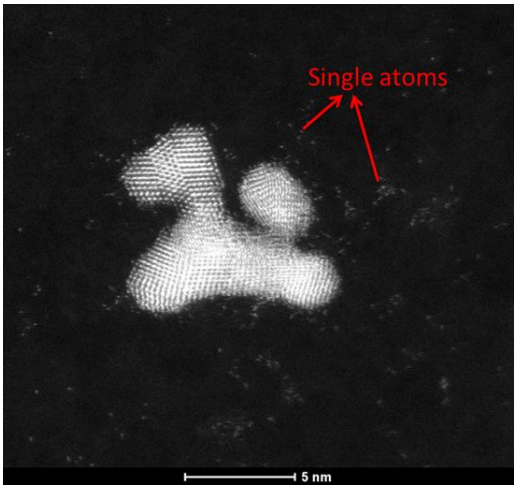

Figure 2. Representative STEM-HAADF image of AuPt nanoparticles showing the presence of single atoms.

In the case of Pt+Au and Au@Pt, EDX maps of individual particles shows the coexistence of Pt and Au elements within the nanoparticle, suggesting the formation of random gold-platinum alloy structures (Figures 2 and 3) with a similar exposition of Au and Pt in both cases.

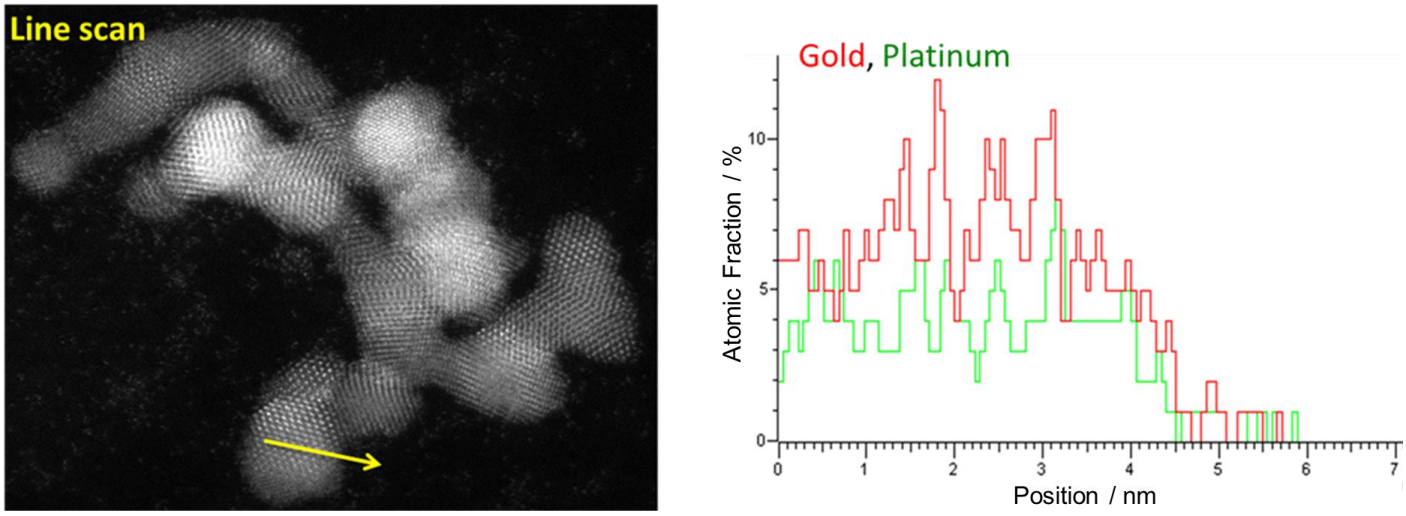

Figure 3. HAADF image of Au+Pt nanoparticles.

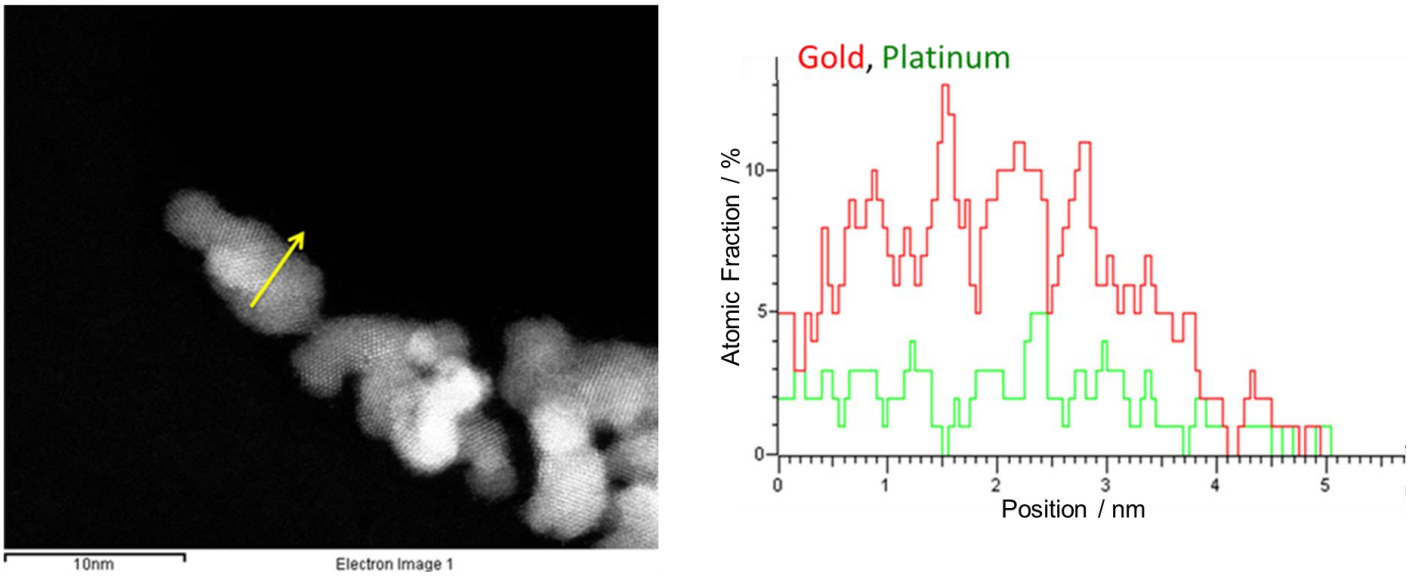

Figure 4. HAADF image a) Pt@Au nanoparticles and b) representative EDX maps of individual particle.

The analysis performed on Pt@Au revealed a different metal disposition from the core to the surface of the nanoparticles. Indeed, the EDX maps showed a Au/Pt ratio enhanced in the central range (core) which decreased significantly when approaching the outer sphere, suggesting a Pt enrichment on the surface (Figure 4).[38-39]

Evolution in time of the Pt@Au system

The peculiar nature of Pt@Au colloidal particles prompted us to study more in detail their evolution, starting from the addition of Pt to the Au pre-formed particles. The fresh system (identified hereafter as "_new") was considered as our time=0, followed by 2, 4 and 24 hours from the reactants addition (identified hereafter as "_2h", "_4h" and "_24h"). It is important to underline that the indicated time is related to the moment in which the solution is deposited on the glassy carbon electrode, and that one additional hour is required to let

the material dry after the deposition on the glassy carbon electrode. Pt and Au monometallic nanoparticle systems were also studied for comparison.

Au(0)NPs are immediately formed and stable in time, presenting oxidation and reduction peaks overlapping for all the solutions (Figure 5).

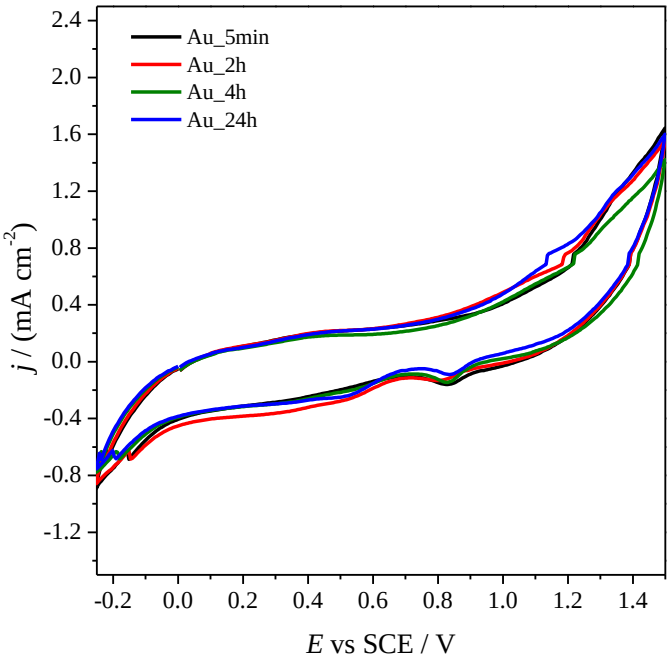

Figure 5. Evolution in time of the monometallic AuNPs system recorded in 0.1 M H_2SO_4 at 100 mV s^{-1}.

In contrast, PtNPs show cyclic voltammograms evolving in time (Figure 6a) reaching a steady-state only after a minimum of 4 hrs. The density current values for both oxidation and reduction peaks, growing from time 0 and time 4hrs, indicated that Pt(0)NPs required more time to be formed with respect to AuNPs. Even after 24 hours, the Pt colloid had not fully reached the final conformation, as evidenced by the still slight shift of the reduction peak potential (Pt_{RED}). This could be relevant especially when Au and Pt are co-reduced (Au+Pt), but in this case the mobility of atoms assures a final state very similar to the system obtained when Pt is reduced first, after which Au is then reduced. Furthermore, the relative faster reduction of Au, allows the system to form a homogeneous alloy.

Bimetallic Pt@Au system (Figure 6b) is formed by reduction of Pt onto Au pre-formed seeds. In this case we could be fairly sure Au is fully reduced before the reduction of Pt take place. In fact, just after the Pt addition (Pt@Au_new), cyclo-voltammetry show both (Au and Pt) reduction peaks, with comparable intensities in terms of current density, meaning that Pt is maintaining its electronic configuration. During this time however, it could be observed that the intensity of Au reduction peak decreased while the Pt one increased. After 2 h of synthesis (Pt@Au_2h) the absence of the gold reduction peak and the decreased density current value of the oxidation plateau suggested the effective formation of the core-shell, in which the internal core made of gold is masked by the external shell of platinum.[39] After 4 h (Pt@Au_4h), the reduction peak relative to gold reappeared slightly cathodically shifted in comparison with AuNPs potential (Au_{RED}), evidencing the tendency of the core-shell to turn into an alloy with the concomitant migration of gold to the surface. This behaviour was also confirmed after 24 hours (Pt@Au_24h). In conclusion, in this system, the

evolution of cyclovoltammetric profiles exclude the segregation of the two metals, but is consistent in terms of gold migration to the surface, thus creating a Au-rich core and a Pt enriched shell with no evidence of segregation of the metals as in an ideal Au core-Pt shell structure (Figure 6c).

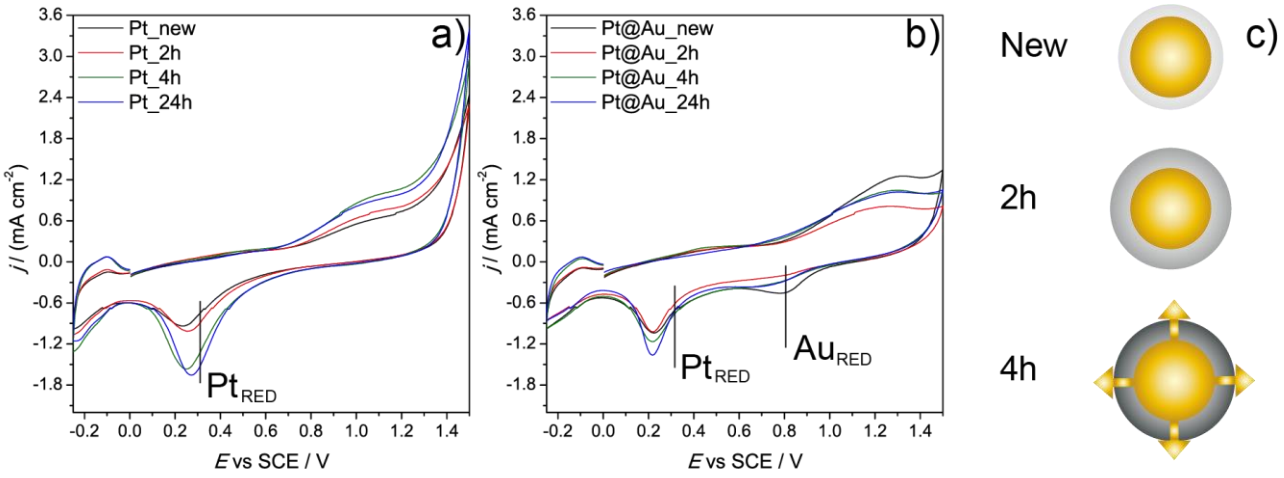

Figure 6. (a)Evolution in time of the monometallic Pt system; (b) Cyclic voltammetry showing the evolution in time of the bimetallic Pt@Au system, with the lines Au_{RED} and Pt_{RED} referring to the ones of Figure 1; (c) Schematic representation of Pt@Au formation.

Another interesting feature of the Pt@Au system is the position of the platinum reduction peak, which remains fixed in time but shifted in comparison with PtNPs potential (Pt_{RED}), probably due to the stabilizing effect of gold, as previously discussed for the final bimetallic structures (Figure 1b).

Conclusions

In the present work, an electrochemical study of bimetallic systems based on Au and Pt nanoparticles (Pt+Au, Au@Pt, Pt@Au) is presented. Cyclic voltammetry has been used as a convenient technique to discriminate between alloyed or core-shell systems, perfect or defective. Moreover, time evolution of the NPs systems has been studied to control the morphology and to give the possibility to fix it at a desired point. This is the first time that CV is used to control and follow the evolution of bimetallic systems in time.

The results show that Pt+Au and Au@Pt behave like alloys with properties different from the monometallic components, and a stabilization of both metal oxides alludes to the intimate contact between Pt and Au. On the other hand, Pt@Au resembles more a core-shell system, particularly at the beginning of its preparation, but tends to be an alloyed system characterized by an enrichment of platinum at the surface. The results obtained by CV, in accordance with those obtained by TEM and UV-Vis techniques, can help researchers to understand the behaviour of these systems in catalysis, electrocatalysis and electroanalytical applications.

Experimental Section

Monometallic systems synthesis

AuNPs by chemical reduction in aqueous solution. 0.031 mmol of solid $NaAuCl_4$ $2H_2O$ (Aldrich, Milan, Italy, 99.99% purity) and polyvinylalcohol solution (PVA, MW(PVA) = 13,000 - 23,000, 87% - 89% hydrolysed, Aldrich; 1% w/w; Au/PVA 1:1, w/w) were added to 100 mL of H_2O. After 3 minutes, $NaBH_4$ (Fluka, Milan, Italy, >96%; Au/$NaBH_4$ 1/4 mol/mol) solution was added to the previous solution under vigorous magnetic stirring. A ruby red Au(0) sol was immediately formed. The sol has been analysed withdrawing samples at 0 min and every 2 hrs.

PtNPs by chemical reduction in aqueous solution. 0.021 mmol of K_2PtCl_4 (Aldrich, Milan, Italy, 99.99 % purity) and polyvinylalcohol solution (PVA, MW(PVA) = 13,000 - 23,000, 87% - 89% hydrolysed, Aldrich; 1% w/w; Pt/PVA 1:1, w/w) were added to 100 mL of H_2O. After 3 minutes, $NaBH_4$ (Fluka, Milan, Italy, >96%; Pt/$NaBH_4$ 1/8 mol/mol) solution was added to the previous solution (yellow-brown coloured) under vigorous magnetic stirring. A black Pt(0) sol was immediately formed. The sol has been analysed withdrawing samples at 0 min and every 2 hrs.

Bimetallic systems synthesis. AuPt nanoparticles (Au:Pt 6:4 molar ratio) were prepared by sol immobiliziation technique using PVA as protecting agent and $NaBH_4$ as reducer. The synthetic procedures are here described in more details.

(Au+Pt) NPs by co-reduction. 0.031 mol of solid $NaAuCl_4$ *$2H_2O$, 0.021 mol of K_2PtCl_4 and PVA solution (1% w/w, metal/PVA 1:1 w/w) were added to 100 mL of H_2O. The yellow solution was stirred for few minutes, after which $NaBH_4$ (metal/$NaBH_4$ = 1/8 mol/mol) solution was added under vigorous magnetic stirring. The sol has been analysed withdrawing samples at 0 min and every 2 hrs.

(Au@Pt) NPs by co-reduction. K_2PtCl_4 (Pt: 0.021 mmol) was dissolved in 40 mL of H_2O and PVA solution (1% w/w) (Pt/PVA= 1:1, wt/wt) was added. The yellow solution was stirred for few minutes, after which $NaBH_4$ (Pt/$NaBH_4$= 1:8 mol/mol) is added under vigorous magnetic stirring. $NaAuCl_4$*$2H_2O$ (Au: 0.031 mmol) was dissolved in 60 mL of H_2O and PVA solution (1% w/w) (Au:PVA= 1:1, wt/wt) was added, under stirring. The solution was then added to the Pt colloidal solution previously prepared and additional $NaBH_4$ (Au:$NaBH_4$= 1:4 mol/mol) was added under vigorous magnetic stirring. The sol has been analysed withdrawing samples at 0 min and every 2 hrs.

(Pt@Au) NPs by co-reduction. $NaAuCl_4$*$2H_2O$ (Au: 0.031 mmol) was dissolved in 60 mL of H_2O and PVA solution (1% w/w) (Au/PVA= 1:1, wt/wt) was then added. The yellow solution was stirred for few minutes, after which $NaBH_4$ (Au/$NaBH_4$= 1:4 mol/mol) was added under vigorous magnetic stirring. K_2PtCl_4 (Pt: 0.021 mmol) will be dissolved in 40 mL of H_2O and PVA solution (1% w/w) (Pt:PVA= 1:1, wt/wt) will be added, under stirring. The solution was then added to the Au colloidal solution previously prepared and additional $NaBH_4$ (Pt:$NaBH_4$= 1:8 mol/mol) was added under vigorous magnetic stirring. The sol has been analysed withdrawing samples at 0 min and every 2 hrs.

Electrochemical measurements. Electrochemical measurements were performed using an AutoLab PGStat30 (EcoChemie, The Netherlands) equipped with the NOVA 2.1 Software. Cyclic Voltammetries (CV) were recorded (at least 5 replicates for each studied system) in a conventional three electrodes cell with a Saturated Calomel Electrode and a Platinum wire used as Reference (RE) and counter (CE) electrodes, respectively. The working electrode (WE) was a glassy carbon one (geometric electrode area = 0.071 cm^2) modified with the different nanoparticle solutions, after being polished with a Struers DP-Nap cloth and synthetic diamond powder (Sigma Adrich). The modified electrode was prepared by drop casting 20 µL of the sought metal nanoparticles colloid using an automatic micropipette (Kartell) and letting it dry for one hour. The CVs were

recorded in an aqueous solution with 0.1 M H_2SO_4 0.1 M as supporting electrolye. The potential was scanned between -0.25 and 1.5 V (SCE) at a scan rate of 100 mV s^{-1}.

In order to follow the evolution in time of the systems, the solutions were drop-casted on the electrode at different synthetic times (just after the start of the synthetic procedure and at two hours intervals) and then, once dried, analysed electrochemically.

HR-TEM analyses. Each sample has been characterized also by TEM. In particular, detailed high resolution High Angle Annular Dark Field Scanning TEM (HAADF-STEM) imaging and energy-dispersive X-ray spectroscopy (EDX) analyses were carried out using FEI Titan 80-300 cubed microscope operated at 200 kV accelerating voltage for a deeper investigation of the AuPt structure. This microscope is equipped with double aberration correctors, providing ultrahigh-resolution HAADF-scanning TEM (STEM) images, and an Oxford Inca energy dispersive X-ray (EDX) spectrometer equipped with a 30 mm^2 ultrathin window Si/Li X-ray detector. EDX data were collected either as spectrum images, in which a focused electron probe was scanned across a region of interest during data collection, or in stationary spot mode, where an emitted X-ray spectrum from 0–20 keV energy range is acquired from a specific point on a particle using a probe size less than 0.5 nm. Spectra were acquired with a probe current of approximately 0.1 nA and dwell times between 200 and 400 ms per pixel, in the case of maps, and 20-30 seconds per analysis in spot mode. STEM HAADF images were acquired using FEI's TIA software and Oxford's INCA microanalysis software was used for EDX acquisition and analysis. The atomic fractions of gold and platinum were quantified by the Cliff-Lorimer method on relative intensities of the Pt-Lα and Au-Lα peaks using k-factors provided by the EDX system manufacturer.

Acknowledgements

Authors thank to Gianluigi A. Botton for the help with TEM characterization of the catalysts.

References

1. Campbell, F. W.; Compton, R. G *Anal. Bioanal. Chem.* **2010**, *396*, 241–259. https://doi.org/10.1007/s00216-009-3063-7
2. Sardar, R.; Funston, A. M.; Mulvaney, P.; Murray, R. W. *Langmuir* **2009**, *25*, 13840–13851. https://doi.org/10.1021/la9019475
3. Rodriguez, J. A.; Goodman, D. W. *Science* **1992**, *257*, 897–903. https://doi.org/10.1126/science.257.5072.897
4. Toshima, N.; Yonezawa, T. *New J. Chem.* **1998**, *22*, 1179–1201. https://doi.org/10.1039/a805753b
5. Ferrando, R.; Jellinek, J.; Johnston, R. L. *Chem. Rev.* **2008**, *108*, 845–910. https://doi.org/10.1021/cr040090g
6. Zaleska-Medynska, A.; Marchelek, M.; Diak, M.; Grabowska, E. *Adv. Colloid Interface Sci.* **2016**, *229*, 80–107. https://doi.org/10.1016/j.cis.2015.12.008
7. Duan, S.; Wang, R. *Progress in Natural Science: Materials International*, **2013**, *23*, 113–126. https://doi.org/10.1016/j.pnsc.2013.02.001

8. Barlocco, I.; Capelli, S.; Zanella, E.; Chen, X.; Delgado, J. J.; Roldan, A.; Dimitratos, N.; Villa, A. *J. Energy Chem.* **2021**, *52*, 301–309. https://doi.org/10.1016/j.jechem.2020.04.031
9. Villa, A.; Wang, D.; Su, D. S.; Prati, L. *Catal. Sci. Technol*. **2015**, *5*, 55–68. https://doi.org/10.1039/C4CY00976B
10. L. Liu; A. Corma, Chem. Rev. **2023,** 123, 4855-4933. https://doi.org/10.1021/acs.chemrev.2c00733
11. Xia, Y.; Xiong, Y.; Lim, B.; Skrabalak, S. E. *Angew. Chem. Int. Ed.* **2009**, *48*, 60–103. https://doi.org/10.1002/anie.200802248
12. Kim, C.; Dionigi, F.; Beermann, V.; Wang, X.; Möller, T.; Strasser, P. *Adv. Mater.* ***2019***, *31*, 1805617 https://doi.org/10.1002/adma.201805617
13. Wu, M.-L.; Chen, D.-H.; Huang, T.-C. *Chem. Mater.* **2001**, *13*, 599–606. https://doi.org/10.1021/cm0006502
14. Hernández-Fernández, P.; Rojas, S.; Ocón, P.; Gómez de la Fuente, J. L.; San Fabián, J.; Sanza, J.; Peña, M. A.; García-García, F. J.; Terreros, P.; Fierro, J. L. G. *J. Phys. Chem. C*, **2007**, *111*, 2913–2923. https://doi.org/10.1021/jp066812k
15. Schrinner, M.; Proch, S.; Mei, Y.; Kempe, R.; Miyajima, N.; Ballauff, M. *Adv. Mater.* **2008**, *20*, 1928–1933. https://doi.org/10.1002/adma.200702421
16. Suntivich, J.; Xu, Z.; Carlton, C. E.; Kim, J.; Han, B.; Lee, S. W.; Bonnet, N.; Marzari, N.; Allard, L. F.; Gasteiger, H. A.; Hamad-Schifferli, K.; Shao-Horn, Y. *J. Am. Chem. Soc.* **2013**, *135*, 7985–7991. https://doi.org/10.1021/ja402072r
17. Bracey, C. L.; Ellis, P. R.; Hutchings, G. J. *Chem. Soc. Rev.* **2009**, *38*, 2231. https://doi.org/10.1039/b817729p
18. Sepúlveda, P.; Rubio, M. A.; Baltazar, S. E.; Rojas-Nunez, J.; Sánchez Llamazares, J. L.; Garcia, A. G. ; Arancibia-Miranda, N. *J. Colloid Interface Sci.*, **2018**, *524*, 177–187. https://doi.org/10.1016/j.jcis.2018.03.113
19. Zhao, B.; Ke, X.-K.; Bao, J.-H.; Wang, C.-L.; Dong, L.; Chen, Y.-W.; Chen, H.-L. *J. Phys. Chem. C* **2009**, *113*, 14440–14447. https://doi.org/10.1021/jp904186k
20. Liu, X.; Wang, D.; Li, Y. *Nano Today*, **2012**, *7*, 448–466. https://doi.org/10.1016/j.nantod.2012.08.003
21. Srnová-Šloufová, I.; Lednický, F.; Gemperle, A.; Gemperlová, J. *Langmuir* **2000**, *16*, 9928–9935. https://doi.org/10.1021/la0009588
22. Beale A. M.; Weckhuysen, B. M. *Phys. Chem. Chem. Phys.* **2010**, *12*, 5562. https://doi.org/10.1039/b925206a
23. Frenkel, A. I. *Chem. Soc. Rev.* **2012**, *41*, 8163. https://doi.org/10.1039/c2cs35174a
24. Baer, D. R.; Amonette, J. E.; Engelhard, M. H.; Gaspar, D. J.; Karakoti, A. S.: Kuchibhatla, S.; Nachimuthu, P.; Nurmi, J. T.; Qiang, Y.; Sarathy, V.; Seal, S.; Sharma, A.; Tratnyek, P. G.; Wang, C. -M. *Surf. Interface Anal.* **2008**, *40*, 529–537. https://doi.org/10.1002/sia.2726
25. Simonsen, S. B.; Chorkendorff, I.; Dahl, S.; Skoglundh, M.; Sehested, J.; Helveg, S. *J. Am. Chem. Soc.* **2010**, *132*, 7968–7975. https://doi.org/10.1021/ja910094r

26. Villa, A.; Dimitratos, N.; Chan-Thaw, C. E.; Hammond, C.; Veith, G. M.; Wang, D.; Manzoli, M.; Prati L.; Hutchings, G. J. *Chem. Soc. Rev.* **2016**, *45*, 4953–4994. https://doi.org/10.1039/C5CS00350D
27. Tschulik, K.; Ngamchuea, K.; Ziegler, C.; Beier, M. G.; Damm, C.; Eychmueller, A.; Compton, R. G. *Adv. Funct. Mater*. **2015**, *25*, 5149–5158. https://doi.org/10.1002/adfm.201501556
28. E. N. Saw; V. Grasmik; C. Rurainsky; M. Epple; K. Tschulik, Faraday Discuss. **2016**, 193, 327. https://doi.org/10.1039/C6FD00112B
29. V. Grasmik; C. Rurainsky; K. Loza; M. V. Evers; O. Prymak; M. Heggen; K. Tschulik; M.Epple, Chem. Eur. J. 2018, 24, 9051 – 9060. https://doi.org/10.1002/chem.201800579
30. Holt, L. R.; Plowman, B. J.; Young, N. P.; Tschulik, K.; Compton, R. G. *Angew. Chem. Int. Ed.* **2016**, *55*, 397–400. https://doi.org/10.1002/anie.201509008
31. L. S. Bezerra; P. Brasseur; S. Sullivan-Allsop; R. Cai; K. N. da Silva; S. Wang; H. Singh; A. K. Yadav; H. L. S. Santos; M. Chundak; I. Abdelsalam; V. J. Heczko; E. Sitta; M. Ritala; W. Huo; T. J. A. Slater; S. J. Haigh; P. H. C. Camargo, Angew. Chem. Int. Ed. **2024**, 63, e202405459. https://doi.org/10.1002/anie.202405459
32. X. Qiu; H. Wei; R. Li; Y. Li, J. J. Alloys Compd. **2023**, 956, 170365. https://doi.org/10.1016/j.jallcom.2023.170365
33. Y. Yu; S. J. Lee; J. Theerthagiri; Y. Lee; M. Y. Choi, Appl. Catal. B: Env. **2022**, 316, 121603. https://doi.org/10.1016/j.apcatb.2022.121603
34. Dimitratos, N.: Messi, C.; Porta, F.; Prati L.; Villa, A. *J. Mol. Catal. A Chem*. **2006**, *256*, 21–28. https://doi.org/10.1016/j.molcata.2006.04.019
35. Peneau, V.; He, Q.; Shaw, G.; Kondrat, S. A.; Davies, T. E.; Miedziak, P.; Forde, M.; Dimitratos, N.; Kiely, C. J.; Hutchings, G. J. *Phys. Chem. Chem. Phys.* **2013**, *15*, 10636. https://doi.org/10.1039/c3cp50361e
36. Tiruvalam, R. C.; Pritchard, J. C.; Dimitratos, N.; Lopez-Sanchez, J. A.; Edwards, J. K.; Carley, A. F.; Hutchings, G. J.; Kiely, C. J. *Faraday Discuss.* **2011**, *152*, 63. https://doi.org/10.1039/c1fd00020a
37. Schwank, J. *Gold Bull.* **1985**, *18*, 2–10. https://doi.org/10.1007/BF03214680
38. Plowman, B. J.; Sidhureddy, B.; Sokolov, S. V.; Young, N. P.; Chen, A.; Compton, R. G. *ChemElectroChem*, **2016**, *3*, 1039–1043. https://doi.org/10.1002/celc.201600212
39. Tschulik, K.; Ngamchuea, K.; Ziegler, C.; Beier, M. G.; Damm, C.; Eychmueller, A.; Compton, R. G. *Adv. Funct. Mater*. **2015**, *25*, 5149–5158. https://doi.org/10.1002/adfm.201501556